Chemical and Water-Isotope Composition Unravels the Source and Evolution of the Kittilä Underground Mine Water, Kiistala, Finland

V. Milesi, J. Declercq, W. Harding, T. Jarman, O. Baas, J. Saukkoriipi, A. van Wageningen, R. Bowell

Chemical and Water-Isotope Composition Unravels the Source and Evolution of the Kittilä Underground Mine Water, Kiistala, Finland

V. Milesi[*,1,2], J. Declercq[2], W. Harding[2], T. Jarman[2], O. Baas[3], J. Saukkoriipi[3], A. van Wageningen[3], R. Bowell[2]

[1]Institut des Sciences de la Terre, Université d'Orléans, Château de la Source, 45100 Orléans, [*]vincent.milesi@univ-orleans.fr; [2]SRK Consulting Ltd (UK), Churchill House, 17 Churchill Way, Cardiff CF10 2HH, UK; [3]Agnico Eagle, Kittilän kaivos, Pokantie 541, 99250 Kiistala, Finland

Abstract

Assessing the environmental impacts of underground mines requires that the mine water sources and the geochemical processes that alter their chemical composition be determined. At the Kittilä underground mine, located near the village of Kiistala in Finnish Lapland, we used chemical and water isotope composition to investigate the contribution of surface and deep water to the mine complex and the source of mine water chlorinity. 39 water samples were collected from surface facilities, rivers, groundwater sources, seeps and drill holes. Four types of water were identified based on chemical composition: a surficial Ca-Mg-HCO_3-type water with low total dissolved solid (TDS) concentrations represented by river and ground waters; a shallow Ca-SO_4-type groundwater represented by seeps, also called 'mine water'; a deep Na-Cl±SO_4-type groundwater sampled from drill holes; and a deep high-Cl brine with a high deuterium enrichment, also collected from drill holes.

Water samples from ponds and underground pumping stations highlight three different mixing processes between the: surficial meteoric low-TDS Ca-Mg-HCO_3-type water and the mine water; mine water and the deep Na-Cl±SO_4-type groundwater and, to a lesser extent; surficial Ca-Mg-HCO_3-type water and the deep Na-Cl±SO_4-type groundwater. In contrast, no evidence of mixing involving the deep high-Cl brines was identified, suggesting that it remains mostly isolated from the other water types.

The hydrogen and oxygen isotope composition of the surficial Ca-Mg-HCO_3-type water and the deep Na-Cl±SO_4-type groundwater, together with chemical evidence of mixing, suggests a possible genetic link between the two endmembers. This is consistent with the presence of the Kiistala shear zone facilitating infiltration by shallow meteoric water into the underlying rock mass and mineralized zone. The negative deuterium excess of the mine water concurrent to sulfate enrichment indicates that it forms from the mixing of surficial Ca-Mg-HCO_3-type water and deep Na-Cl±SO_4-type groundwater that evolved through evaporation and sulfide oxidation. A mixing ratio of 80% of the surficial Ca-Mg-HCO_3-type water and 20% of the deep Na-Cl±SO_4-type groundwater best explains the Cl concentration of the mine water. The linear relationship between the sulfate concentrations of the mine waters and its isotopic deviation from the Global Meteoric Water Line suggests a correlation between evaporation and sulfide oxidation at Kittilä, which could represent a new tool for the assessment of water-rock reactions.

Introduction

Management of water quality is a major challenge during mine operations and after closure. The quality of any groundwater and surface water leaving a mine site is subject to stringent and enforceable standards. Therefore, better knowledge of the processes that control the chemistry of mine waters enables long-term water management planning to avoid regulatory infractions.

Underground mines are especially complex systems as they usually involve several sources of water to the mine, including surface water, groundwater, seepage from overlying active pits or pit lakes, coupled with chemical weathering involving highly reactive rocks from exposed tunnel surfaces or backfilled rocks. Thus, mine water is not immediately derived from precipitation or from rapid and direct infiltration (Douglas et al. 2000; Gammons et al. 2006; Walton-Day and Poeter 2009) but results from the interplay of several geochemical processes.

Due to the conservative nature of the stable isotope composition of water within an aquifer, water isotopes can be used to trace water origin. Except when exposed to temperatures >60–80 °C (D'amore and Panichi 1985), groundwater retains its initial isotopic composition for thousands of years. Therefore, when two isotopically distinct water sources mix into a common pool, isotopes can be used to quantify the contribution of each initial source through mass balance calculation (Faure and Mensing 2005). Several processes, however, can produce isotopic fractionation. High evaporation rates in tailing ponds produce large isotopic fractionation (Gammons et al. 2006), but the extent of this mechanism in underground environments is unclear due to high humidity levels (Ersek et al. 2018). Water-rock reactions can also produce isotopic fractionation when associated with either high temperatures (Bowers and Taylor 1985) or low-temperatures and high rock/water ratios (Clark and Fritz 2013; Warr et al. 2021) (Fig. 1); however, those conditions are unlikely to prevail in chemical weathering related to underground mining activities. Few studies have analyzed water isotopes in underground mine waters and of those that have, several focused on a single site (Gammons et al. 2006, 2009, 2010; Pellicori et al. 2005). Expanding the water isotope dataset of underground mines allows a better understanding of how they can be used to track water sources and geochemical processes.

The Kittilä underground mine is developed within a mafic metavolcanics rock formation (the Kittilä Group), along the Kiistala shear zone trending N-S to NNE-SSW. The occurrence of pervasively fractured rocks within the shear zone could affect the hydraulic connection between the mine complex, the surface waters, and deep saline formation waters previously identified in the Fennoscandian Shield (Kietäväinen et al. 2013; Nurmi et al. 1988). In 2016, the Geological Survey of Finland used the water (H and O), Sr, and S-SO_4 isotope and chemical compositions of the Kittilä underground mine waters to identify five potential sources of water reporting to the mine complex: surface water derived from the nearby Seurujoki River, meteoric groundwater either affected or not by mining activity, process water, and deep saline formation water (Papp et al. 2018). Using qualitative interpretation of water endmembers combined with a quantitative isotope mixing model, the authors suggested that most underground mine dewatering water was of meteoric groundwater origin, but that there were also influences from both the Seurujoki River and the deep saline formation water. To better characterize the water sources and refine the mixing models, the influence of geochemical processes on the isotopic signature must be assessed, as they could also cause the variation of water isotopic composition shown in Fig. 1.

Figure 1 should be placed near here during the final printing process.

Here, we report the chemical and isotopic (H and O) composition for a large set of water samples and compare the data with isotopic fractionation models. Our objectives were specifically to assess the connection of the mine complex with surface waters and the source of mine water chlorinity. Our results show how the combination of water chemistry and isotopic data in an underground mine environment allows the characterization of water endmembers, their contribution to the mine water, and the geochemical processes that control their composition.

Mine Site and Geologic Settings

The Kittilä mine (also known as the Suurikuusikko mine) is a gold mine 36 km north-east of Kittilä, in the Lapland County of Finland. The mine has operated since 2008 and consists of two open pits and an underground mining operation that uses both transverse and longitudinal long-hole stoping methods. Since the closure of open pit mining in 2012, the Kittilä mine has been an underground operation only.

The main bedrock lithology at Kittilä consists of the ca 2.0 Ga Kittilä Group rocks (Luukas et al. 2017), which is part of the volcano-sedimentary succession of the Paleoproterozoic Central Lapland Greenstone Belt of northern Finland. It is 6–9 km thick over > 2600 km^2 (Hanski and Huhma 2005) and consists of Fe- to Mg-tholeiitic basalts, plagioclase porphyry felsic intrusions, banded iron formations, and metasedimentary packages including metagreywackes, phyllites, and graphite- to sulphide-bearing schists. Sulfide minerals, mainly pyrite and arsenopyrite, are generally present throughout the different lithologies, although the BIF contains the largest proportion of pyrite (up to 91%).

The supracrustal rocks in the Kittilä Group have been divided into four formations (Lehtonen et al. 1998). The Porkonen Formation where the Kittilä mine is located is a transitional zone between the Kautoselka and Vesmajarvi formations and comprises mafic tuffs, graphitic metasedimentary rocks, black chert, and banded iron formation (BIF) (Fig. 2). It varies in thickness between 50 and 200 m and is characterized by strong heterogeneous penetrative strain, narrow shear zones, breccia zones, and intense hydrothermal alteration (carbonate-albite-sulfide). The metamorphic grade is greenschist facies, accompanied by carbonate, chlorite, sericite, and albite alteration, especially along the Kiistala and Sirkka shear zones (Hölttä et al. 2007). The ore deposit is hosted within the Kiistala shear zone, which is the main regional feature locally trending N-S to NNE-SSW. The ore lenses are located predominantly within a strongly sheared envelope, where the rock is pervasively fractured down to 100-200 m of depth.

At surface, the bedrock is covered by a thin (2-7 m thick) veneer of mixed glacial tills, which is overlain by a wetland peat habitat (1-2 m thick) in the lower lying areas. Where peats and silts are absent, the overburden allows rapid recharge of water into the shallow groundwater system, especially following the spring snow melt and after significant precipitation events. Weathered bedrock occurs to a depth of about 25-30 m and is characterized by increased fracturing and a poor rock-mass quality compared with the underlying fresh bedrock. The vertical faults within the Kiistala shear zones are the most significant hydrogeological features in terms of inflow contributions. The dewatering rate for the mine in the period 2019-2020 ranged between 650 and 850m^3/hour. Dewatering of the mine has induced a downward hydraulic gradient within the shear zone, which is expected to increase with time as the mine is deepened and dewatering progresses.

Figure 2 should be placed near here during the final printing process.

Methods

Samples were collected during two sampling campaigns, the first performed by the Geological Survey of Finland (GTK) in 2015 and the second by SRK Consulting in 2021. The 2015 data are published in an open-access GTK work report (Papp et al. 2018). For the 2021 SRK campaign, the sampling locations were selected to represent a large diversity of samples in terms of depth, mine areas (Rimpi, Roura, Suuri, research tunnels), and water types (river, groundwater, seepage, ponds, pumping station, drill hole; supplemental Table S-1). The analysis of major and trace element compositions was carried out at Eurofins laboratory with atomic emission spectroscopy and inductively coupled plasma mass spectrometry. The samples of the deep saline formation water were diluted for analysis. Estimated uncertainties are of ±0.1 unit for pH, ±3% for major cations and anions, and ±5% for trace elements. The oxygen and hydrogen isotope composition of water was measured at the laboratory of the Geological Survey of Finland (GTK) with cavity ring down spectroscopy (CRDS), Picarro L2130-i. Vaporized water sample was led into a pressure and temperature controlled optic chamber, where the amounts of oxygen and hydrogen isotopes were measured with an infrared laser. Isotope ratios of oxygen and hydrogen are reported using the δ notation, which represents as per mil the difference of the $^{18}O/^{16}O$ or $^{2}H/^{1}H$ ratio, R, of the sample with the international standard, VSMOW, such that:

$$\delta = \left(\frac{R_{sample}}{R_{VSMOW}} - 1\right) * 1000.$$

Hereafter, the oxygen and hydrogen isotope composition are referred to $\delta^{18}O$ and δD, where D stands for deuterium, ^{2}H. The uncertainty of measurement is < 0.1‰ for oxygen analysis and < 0.3‰ for hydrogen analysis. The assessment of duplicates, field blank, and the ionic balance highlighted the quality of the analysis (see supplemental Figs. S-1 to S-3 in the supporting information).

Results

Chemical Composition

The chemical composition of water samples is presented in Piper diagrams as a function of ionic strength and depth (Fig. 3a and b). The complete dataset is provided in File S-1 in supporting information. Four endmembers are identified:

- Ca-Mg-HCO_3-type water with low ionic strength, represented by surface water (i.e. up-stream river and groundwater)
- Ca-SO_4-type groundwater with high ionic strength, also called ‘mine water’, represented by seeps at depth ranging from surface to ≈ 600 m

- Na-Cl±SO_4-type groundwater with moderate ionic strength, represented by waters from some drill holes below 600 m of depth
- high-Cl brine with a very high ionic strength (Cl concentration up to 60,000 mg/L), represented by waters from some of the drill holes below 700 m of depth

Figure 3 should be placed near here during the final printing process.

Several samples plot between the water endmembers identified. Some samples of the groundwater, downstream river, seepage, underground pumping station, and drill holes plot between the surficial Ca-Mg-HCO_3-type water and the mine water. Water samples from the underground pumping station and ponds have chemical composition between the mine water and the deep Na-Cl±SO_4-type groundwater. Sulphate concentrations of up to 6000 mg/L in one of the ponds highlight the dominant contribution of mine water. Finally, a few samples from seepage and drill hole sources display a chemical composition between the deep Na-Cl±SO_4-type of groundwater and the surficial Ca-Mg-HCO_3-type water. The 2015 and 2021 samples are consistent in terms of water endmembers.

Cross Section

The Kittilä underground mine is developed along the Kiistala shear zone trending N-S to NNE-SSW, so it is possible to represent the chemical composition of water in a 2D space, Depth vs. Northing. Although the extrapolation calculation of the chemical composition between samples is driven by the sample distribution, this representation is useful in visualizing the spatial variation of water chemistry across the mine. Overall, the Cl concentration increases from ca. 1 mg/L at surface to 1,000 mg/L at depth (Fig. 4a). The high-Cl brine with concentrations up to 60,000 mg/L occurs abruptly below 800 m depth in the northern section, i.e. the RIMPI area. In the 2015 dataset, the high-Cl brine was reported at ca. 700 m of depth, i.e. a shallower depth than in 2021 (ca. 1000 m), which must be considered in the scope of the mine development. The high-Cl brine is depleted in SO_4 and enriched in Mn and H_2S (Fig. 4b, c, and d). In the mine waters (Ca-SO_4-type) collected from seepage and pumping stations between 100 and 600 m of depth, the high sulfate concentrations are strongly correlated with Mn (Fig. 4d). The saturation index for gypsum and calcite shows that the mine water is at equilibrium with calcite and gypsum, whereas the surficial Ca-Mg-HCO_3 water, the deep Na-Cl±SO_4-type groundwater, and the deep high-Cl brine are undersaturated (Fig. 4e and f).

Figure 4 should be placed near here during the final printing process.

Oxygen and Hydrogen Water Isotopes

Isotopic composition

The hydrogen and oxygen isotope composition of the water samples are represented in a δD vs $\delta^{18}O$ plot as a function of Cl and sulfate concentration (File S-**1** in supporting information and Fig. 5). The sample compositions are compared to the Global Meteoric Water Line (GMWL), which better fit the data than local meteoric water lines (see Fig. S-4 in supporting information, Craig 1961). Samples of river, groundwater, and deep waters collected from seepage and drill hole at < 600m of depth plot on the GMWL with $\delta^{18}O$ and δD values ranging from -15.5‰ to 14‰ and -112‰ to -102‰, respectively. Among these samples, the river and groundwater samples have low Cl and sulfate concentrations and correspond to the surficial Ca-Mg-HCO_3-type water (Fig. 5a and b). The samples from underground drill holes have substantial amounts of Cl and sulfate and represent the deep Na-Cl±SO_4-type groundwater.

Figure 5 should be placed near here during the final printing process.

Three samples show very high enrichment in deuterium with δD values ranging from -85‰ to -60‰ (Fig. 5). These samples have Cl concentrations up to 60,000 mg/L and low sulfate concentrations and correspond to the high-Cl brine collected at high depth (> 700m). They form a linear trend with the Ca-Mg-HCO_3-type water and the Na-Cl±SO_4-type groundwater on the GMWL.

Most waters from underground seepages, pumping stations, and ponds deviate from the GMWL according to a trend corresponding to a negative deuterium excess (Fig. 5). They have high sulfate concentrations and moderately high Cl concentrations, between the Cl concentration of ca. 1 mg/L of the surficial Ca-Mg-HCO_3-type water and the ca. 100 mg/L of the deep Na-Cl±SO_4-type groundwater (Fig. 5a and b). These waters correspond to the shallow Ca-SO_4-type groundwater, i.e. the mine water. Fig. 6 shows the isotopic distance of samples to the GMWL as a function of the sulfate concentration. The isotopic deviation is strongly correlated to the sulfate enrichment; the further the samples are from the GMWL, the higher their sulfate concentrations. The mine water represented by the underground seepages, pumping stations, and ponds shows the greatest isotopic fractionation, associated with the highest sulfate concentrations, above 1,000 mg/L.

Figure 6 should be placed near here during the final printing process.

Isotopic fractionation model

In addition to the isotopic fractionation processes presented in Fig. 1, which were considered qualitatively to interpret our dataset (see Discussion section below), two isotopic fractionation processes were evaluated quantitatively. The formation of ice from water results in a D and ^{18}O enrichment of the ice (Ersek et al. 2018; Lehmann and Siegenthaler 1991). The ice endmember has a negative deuterium excess compared to the GMWL. Given the monthly average temperature at Kittilä < 0°C from October to April, ice melting during the spring season could represent a substantial input of water with an isotopic signature shifted from the GMWL. When water sources mix and the resulting mixture does not undergo isotopic fractionation, isotopes can be used to quantify the contribution of each initial source using the mass balance equation (Faure and Mensing 2005):

$$\delta_{pool} = [n\delta_{source1}] + [(1-n)\delta_{source2}]$$

An isotopic mixing model was calculated considering the surface waters and the water produced by ice melting as the two endmembers (Fig. 5). The average isotopic composition of the surface waters from the 2021 samples (i.e. the river and the groundwater) was considered in the calculation, that is δD and $\delta^{18}O$ values of -108.3‰ and -14.8, respectively. The ice-water isotopic fractionation was taken from the study of Lehmann and Siegenthaler (1991) ($\Delta D_{ice\text{-}water}$ from +17 to +21 and $\Delta O_{ice\text{-}water}$ from +2.6 to +2.9‰) so that the isotopic signature of the ice endmember ranges from -93‰ to -89‰ for δD and -11.9‰ to 12.2‰ for $\delta^{18}O$. During mixing, the δD and $\delta^{18}O$ values of the mixture increase with the contribution of melted ice; however, the model offers little consistency with the data.

Craig (1961) established the relationship between $\delta^{18}O$ and δD during an evaporation process. This model was applied, considering as the initial water body (before any evaporation) the average isotopic composition of the surface waters from the 2021 samples (Fig. 5). Compared to the GMWL, evaporation results in a negative deuterium excess that follows the same isotopic trend as the one displayed by the mine waters.

Gonfiantini et al. (1986) developed a refined evaporation model that allows determination of the isotopic composition of an evaporated water body as a function of the evaporation rate and the relative humidity. Deviation of the isotopic composition from the GMWL increases with increasing evaporation rate and decreasing relative humidity (Fig. 5). The mine waters are consistent with an evaporation rate ranging from 0 to 10% at a relative humidity of 70-80%.

Discussion

Water Endmembers and Mixing

Four water endmembers were identified based on their chemical and isotopic compositions, depth, and sample type: surficial Ca-Mg-HCO_3-type water; shallow Ca-SO_4-type groundwater, also called mine water, deep Na-Cl±SO_4-type groundwater, and deep high-Cl brine. The correlation between the Mn and sulfate concentrations in the mine water supports the oxidative dissolution of polymetallic sulfides as the main source of sulfate. The high mineralization results in equilibrium with calcite and gypsum, the precipitation of which controls the Ca and sulfate composition of the mine waters.

The density of samples with chemical compositions between the identified water endmembers highlights the mixing processes. Samples from mine groundwater, down-stream river, some seepages, and some pumping stations clearly show mixing between the surficial Ca-Mg-HCO_3-type water and the mine water. Waters from the pumping stations and ponds also highlight mixing between the mine water and the deep Na-Cl±SO_4-type groundwater. To a lesser extent, a few seepage and drill hole samples likely indicate mixing between the surficial Ca-Mg-HCO_3-type water and the deep Na-Cl±SO_4-type groundwater. This latter mixing is consistent with the Kiistala shear zone hydrogeological properties, which likely enables infiltration of the surface water to depth. Furthermore, the isotopic composition of the surficial Ca-Mg-HCO_3-type water and the deep Na-Cl±SO_4-type groundwaters are relatively similar and are both consistent with the GMWL; this supports a possible connection between the two water reservoirs. If correct, the deep Na-Cl±SO_4-type groundwater may have derived from the surficial Ca-Mg-HCO_3-type water and may evolve into a more mineralized Na-Cl±SO_4-type groundwater along the infiltration flow path, while keeping a relatively constant isotopic composition. The sulfate enrichment of the deep Na-Cl±SO_4-type groundwater compared to the surficial Ca-Mg-HCO_3-type water is consistent with the oxidation of polymetallic sulfide during infiltration. Age dating would bring further constraints on the connection between the surficial Ca-Mg-HCO_3-type water and the deep Na-Cl±SO_4-type groundwater.

Origin of the Deep High-Cl Brine

Our isotopic data does not show any evidence of mixing between the deep high-Cl brine with D enrichment and the mine water (i.e. shallow Ca-SO_4-type groundwater); however, the linear isotopic trend formed by the deep high-Cl brines with the surficial Ca-Mg-HCO_3-type water and the deep Na-Cl±SO_4-type groundwater may indicate a mixing process. Mixing between local meteoric water and deep deuterium-enriched brines was reported for instance in the principal Canadian Shield mining camps (Fritz and Frape 1982). If this is the case at Kittilä, the rare occurrence of samples representing mixing and their high D and Cl enrichments highlights a poor connection between the two endmembers.

The deep high-Cl brine was collected at ca. 700 m of depth in 2015 and ca.1100 m of depth in 2021. This suggests that the brine occurs in isolated pockets of highly mineralized ancient water, only occasionally intercepted by the operation in the deeper regions of the mine and, therefore it does not contribute significantly to the mine water budget. This is supported by the high H_2S and high Mn concentrations, which could result from equilibrium of water with polymetallic sulfide minerals in a closed reducing environment. Such deep brine waters, enriched in Cl and deuterium, have previously been identified in the Fennoscandian Shield (Kietäväinen et al. 2013; Nurmi et al. 1988) and in other settings, such as the German continental deep drill hole (Lodemann et al. 1998). Their isotopic signatures were interpreted as being the result of low-temperature hydration of primary silicates where the water-rock ratio is very low and spans extended geological time scales (Kietäväinen et al. 2013; Lodemann et al. 1998). High H_2S concentrations, as observed in our samples, could also produce an increase of the δD of water through deuterium exchange with water (Clark and Fritz 2013). It is likely that the observed isotopic signature is the product of both processes.

Mine Water Source and Evolution

Several geochemical processes can produce the negative D excess observed in the mine water. Based on the water samples collected in 2015, Papp et al. (2021) attributed this water isotope composition of the mine water to accelerated water-rock reactions or to fractionation that occurs during the mineral beneficiation process, related to flotation. As reported in Fig. 1, several geochemical processes can lead to the fractionation of water isotopes. At temperature above 200°C, water-rock reactions result in ^{18}O exchange between ^{18}O-depleted water and ^{18}O-enriched minerals whereas the deuterium content of the thermal water remains unchanged due to the low hydrogen content of the rock-forming minerals (e.g. Bowers and Taylor 1985). In sedimentary formations, ^{18}O and D enrichment can also result from a combination of processes including ^{18}O exchange with carbonate minerals at high temperature (Clayton et al. 1966), deuterium exchange with hydrocarbons, H_2S, and hydrated minerals, dewatering of clays during compaction, hydration of anhydrite (Bath et al. 1987), and hyperfiltration in low permeability formation (Phillips and Bentley 1987). Oxygen exchange between sulfate and H_2O is another possible process known to occur rapidly at temperatures above 200 °C; however, its half-life increases exponentially below 150 °C to reach > 10 Myrs at normal groundwater temperature (Chiba and Sakai 1985). None of these processes is consistent with the mafic metavolcanic rocks at Kittilä, nor with the low temperatures of ca. 10 °C in the underground mine (see Fig. S-5 in supporting information). The isotopic data is not consistent with an input of water produced by ice melting with a negative deuterium-excess, as has been observed in cave drip waters (Ersek et al. 2018).

Instead, the isotopic composition of the mine water is best explained by an evaporative process. The effect of evaporation on mine waters has been previously reported and used to quantify the evaporation rate of pit lake and tailing ponds with relatively high evaporation rate from 12 to 60% (Gammons et al. 2006, 2009, 2010; Pellicori et al. 2005; Singh et al. 2018). These evaporation rates that occur on open waters are much higher than those inferred from our isotopic dataset in the Kittilä underground mine. Our study indicates a low evaporation rate of 0 to 10% at a high relative humidity of 70-80%, which is consistent with previous studies in underground environments (e.g. Ersek et al. 2018). Gammons et al. (2006) showed that the intersection of the mine water evaporation trend with the GMWL can be used to calculate the average water isotope composition of the recharge water to the mine complex. At the Kittilä underground mine, the recharge water isotope signature is consistent with both the surficial Ca-Mg-HCO_3-type water and the deep Na-Cl±SO_4-type groundwater, as these two water endmembers have a similar isotopic composition. Whilst the isotope dataset does not allow us to assess the contribution of each of the water sources to the mine complex, it is enough to show that the mine water derives from one of these two water sources, or a combination of both. A more in-depth assessment of the contribution of water sources to the mine is provided hereafter using a mixing model based on Cl concentration.

Correlation Between Sulfate Concentrations and Water Isotopes

Our dataset shows a strong correlation between the sulfate concentration of the mine water and its isotopic deviation from the GMWL. A possible hypothesis to explain this trend is that as water interacts with the rock in the Kittilä underground mine, the evaporation rate and the extent of sulfide oxidation progress synchronously. Because evaporation as a physical process and sulfide oxidation as a chemical process are basically separated, the apparent correlation between these two reactions must result from underlying mechanisms including pathway of seepages in the fracture network or in the underground tunnels. Especially, the correlation could result from the operating parameters of the mine ventilation system, which would control both air flow and oxygen concentration, i.e. the key parameters for evaporation underground and sulfide oxidation, respectively. If correct, this would indicate that evaporation does not occur in between the water source and its infiltration to the mine. This would also suggest that sulfide oxidation occurs in the open mine workings rather than in water-filled fractures where evaporation could not proceed.

An alternative explanation to the correlation between the sulfate enrichment and the water isotope deviation in the mine water is mixing between the surface water and a hypothetical mine water endmember characterized by high rates of evaporation and sulfide oxidation. However, this hypothesis is difficult to reconcile with the spatial distribution of the mine water samples (i.e. seep samples mostly; Fig. 4). Moreover, the formation of the mine water endmember through a reaction pathway involving increased evaporation and sulfide oxidation rates would produce intermediate degrees of less evolved mine water along the way, which is equivalent to our first hypothesis. Following Occam's razor principle that the explanation that requires the fewest assumptions is the most likely, we propose that our data are best explained by the synchronous evolution of evaporation and sulfide oxidation in the Kittilä underground mine.

Deeper investigations of the underlying mechanisms are necessary to confirm the apparent physico-chemical correlation between evaporation and sulfide oxidation at Kittilä. If confirmed, the relationship between the two processes opens the way to a new use of water isotopes as a geochemical tracer. Especially, changes in the correlation between water isotopes and sulfate concentration at Kittilä could be used to assess the efficiency of measures taken to avoid contact of mine water inflows with oxygen.

Mine Water Balance

Our results are consistent with the study of Papp et al. (2021) in the identification of the different water sources to the mine. Those authors suggested that most of the underground mine dewatering water was of meteoric groundwater origin, but that there were influences of the Seurujoki River and deep saline formation water as well. Our isotopic dataset does not allow us to quantify the relative contribution of these water sources because of the similar isotopic composition between the groundwater and river water. Therefore, Cl was used as a conservative tracer to develop mixing models between the water endmembers. Two mixing scenarios can explain the Cl concentrations of the mine water: (1) a mixing of surficial Ca-Mg-HCO_3-type water with deep Na-Cl±SO_4-type groundwater or (2) a mixing of surficial Ca-Mg-HCO_3-type water with deep high-Cl brine. The effect of the evaporation rate is negligible in these calculations. In the first mixing scenario, the contribution of the deep Na-Cl±SO_4-type groundwater to the mine water is ca. 25±5%, whereas in the second scenario, the contribution of the deep high-Cl brine is 0.05±0.01%. These conservative mixing models confirm the poor connection of the deep high-Cl brine with the other water endmembers. Although the second mixing scenario cannot be ruled out based on our dataset, the very low mixing ratio that it implies makes it unlikely. Therefore, the surficial Ca-Mg-HCO_3-type water and the deep Na-Cl±SO_4-type groundwater appear to be the main sources of water in the Kittilä underground mine, whereas the deep high-Cl brine remains relatively isolated. The dominant contribution of the surficial Ca-Mg-HCO_3-type water is consistent with the downward hydraulic gradient within the Kiistala shear zone that results from the mine dewatering. The systematic occurrence of deep high-Cl brines in the deepest part of the mine from 2015 to 2021 suggests that their contribution to the mine water balance could increase as the mine is deepened. It could, however, be counterbalanced by the increased downward hydraulic gradient as mine dewatering keeps progressing.

Conclusion

The chemical and isotopic composition (oxygen and hydrogen) of water samples from the Kittilä underground mine was analyzed to constrain the water sources and their contributions to the mine. Four water endmembers were identified:

- a surficial Ca-Mg-HCO_3-type water represented by river and ground waters
- a shallow Ca-SO_4-type groundwater captured in seepages also called mine waters
- a deep Na-Cl±SO_4-type groundwater collected from drill holes
- a deep high-Cl brine collected from drill holes with a high deuterium anomaly

Water samples from ponds and underground pumping stations highlight substantial mixing between: the surficial Ca-Mg-HCO_3-type water and the mine water; the mine water and the deep Na-Cl±SO_4-type groundwater; and possibly between the surficial Ca-Mg-HCO_3-type water and the deep Na-Cl±SO_4-type groundwater.

The similar isotopic composition of the deep Na-Cl±SO_4-type groundwater and the surficial Ca-Mg-HCO_3-type water, together with chemical evidence of mixing, suggest a genetic link between the two endmembers on a geologic time scale, i.e. not related to mining activities. The Kiistala shear zone may have facilitated infiltration of surface water to depths where it was enriched in sulfate through sulfide oxidation along its path through the bedrock, whereas the isotopic composition remained unchanged, i.e. on the GMWL. Our isotopic dataset does not allow us to determine the relative contributions of groundwater and river water to the surficial Ca-Mg-HCO_3-type water due to their similar isotopic compositions.

Deviation of the water isotope composition of the mine water away from the GMWL in parallel to sulfate enrichment suggests that the mine water is derived from a mixture of surficial Ca-Mg-HCO_3-type water and deep Na-Cl±SO_4-type groundwater that evolved through evaporation and sulfide oxidation. The linear relationship between the sulfate concentration and the negative deuterium excess of the mine water could indicate that evaporation and sulfide oxidation occur concurrently. Although a deeper investigation of underlying mechanisms is required, this apparent physico-chemical correlation, if correct, suggests that water isotopes could represent a new tool to assess the efficiency of measures taken to avoid contact of mine water inflows with oxygen.

A mixing ratio of 75% of surficial Ca-Mg-HCO_3-type water and 25% of deep Na-Cl±SO_4-type groundwater best explains the Cl concentration of the mine water, which is consistent with the downward hydraulic gradient within the shear zone. On the other hand, the deep high Cl-brines enriched in deuterium are poorly connected with the other water endmembers. Despite the large deuterium enrichment of the deep high-Cl brine, which would allow us to distinguish even low mixing ratios, the isotopic data does not show any evidence of mixing with the mine water. In addition, if the brines were to be involved as a water source to the mine, an unlikely ratio of 99.95% of surface water and 0.05% of deep high-Cl brines would be required to explain the Cl concentration of the mine water. Although the deep high-Cl brines are currently poorly connected to the mine, its systematic occurrence at depth in 2015 and 2021 suggests that further deepening of the mine could increase its contribution to the mine water budget.

Acknowledgments: We are grateful to Agnico Eagle Mines Ltd and SRK Consulting Ltd (UK) for their support in publishing this study. We also thank the editors and four anonymous reviewers for their comments, which greatly contributed to improving the manuscript.

References

Bath AH, Darling WG, George IA, Milodowski AE (1987) $^{18}O^{16}O$ and $^{2}H^{1}H$ changes during progressive hydration of a Zechstein anhydrite formation. Geochim Cosmochim Acta 51(12):3113–3118

Bowers TS, Taylor HP (1985) An integrated chemical and stable-isotope model of the origin of Midocean Ridge Hot Spring Systems. J Geophys Res 90(B14):12583. doi.org/10.1029/JB090iB14p12583

Chiba H, Sakai H (1985) Oxygen isotope exchange rate between dissolved sulfate and water at hydrothermal temperatures. Geochim Cosmochim Acta 49(4):993–1000

Clark ID, Fritz P (2013) Environmental Isotopes in Hydrogeology, CRC Press

Clayton RN, Friedman I, Graf DL, Mayeda TK, Meents WF, Shimp NF (1966) The origin of saline formation waters: 1. Isotopic composition. J Geophys Res 71(16):3869–3882

Craig H (1961) Isotopic variations in meteoric waters. Science 133(3465):1702–1703

D'amore F, Panichi C (1985) Geochemistry in geothermal exploration. Int J Energy Res 9(3):277–298. doi.org/10.1002/er.4440090307

Douglas M, Clark ID, Raven K, Bottomley D (2000) Groundwater mixing dynamics at a Canadian Shield mine. J Hydrol 235(1–2):88–103. doi.org/10.1016/S0022-1694(00)00265-1

Ersek V, Onac BP, Perșoiu A (2018) Kinetic processes and stable isotopes in cave dripwaters as indicators of winter severity. Hydrol Process 32(18):2856–2862. doi.org/10.1002/hyp.13231

Faure G, Mensing TM (2005) Isotopes: Principles and Applications. John Wiley & Sons, Inc

Fritz P, Frape SK (1982) Saline groundwaters in the Canadian Shield—a first overview. Chem Geol 36(1–2):179–190

Gammons CH, Brown A, Poulson SR, Henderson TH (2013) Using stable isotopes (S, O) of sulfate to track local contamination of the Madison karst aquifer, Montana, from abandoned coal mine drainage. Appl Geochem 31:228–238. doi.org/10.1016/j.apgeochem.2013.01.008

Gammons CH, Duaime TE, Parker SR, Poulson SR, Kennelly P (2010) Geochemistry and stable isotope investigation of acid mine drainage associated with abandoned coal mines in central Montana, USA. Chem Geol 269(1–2):100–112. doi.org/10.1016/j.chemgeo.2009.05.026

Gammons CH, Poulson SR, Pellicori DA, Reed PJ, Roesler AJ, Petrescu EM (2006) The hydrogen and oxygen isotopic composition of precipitation, evaporated mine water, and river water in Montana, USA. J Hydrol 328(1–2):319–330. doi.org/10.1016/j.jhydrol.2005.12.005

Gammons CH, Snyder DM, Poulson SR, Petritz K (2009) Geochemistry and Stable Isotopes of the Flooded Underground Mine Workings of Butte, Montana. Econ Geol 104(8):1213–1234. doi.org/10.2113/gsecongeo.104.8.1213

Gonfiantini R (1986) Environmental isotopes in lake studies. Ch. 3 in: Fritz P (Ed.), The Terrestrial Environment, Elsevier, pp 113–168. doi:10.1016/B978-0-444-42225-5.50008-5

Hanski E, Huhma H (2005) Central Lapland greenstone belt. Ch. 4 in: Lehtinen M, Nurmi PA, Rämö OT (Eds.), Precambrian Geology of Finland Key to the Evolution of the Fennoscandian Shield, vol 14, Developments in Precambrian Geology, Elsevier, pp 139–193. doi.org/10.1016/S0166-2635(05)80005-2

Hölttä P, Väisänen M, Väänänen J, Manninen T (2007) Paleoproterozoic metamorphism and deformation in Central Lapland, Finland. Gold Cent Lapland Greenstone Belt Geol Surv Finl Spec Pap 44: 7-56

Kietäväinen R, Ahonen L, Kukkonen IT, Hendriksson N, Nyyssönen M, Itävaara M (2013) Characterisation and isotopic evolution of saline waters of the Outokumpu Deep Drill Hole, Finland–implications for water origin and deep terrestrial biosphere. Appl Geochem 32:37–51

Lehmann M, Siegenthaler U (1991) Equilibrium oxygen-and hydrogen-isotope fractionation between ice and water. J Glaciol 37(125):23–26

Lehtonen MI, Airo ML, Eilu P, Hanski E, Kortelainen V, Lanne E, Manninen T, Rastas P, Räsänen J, Virransalo P (1998) The stratigraphy, petrology and geochemistry of the Kittilä greenstone area, northern Finland. A Report of the Lapland Volcanite Project. Geological Survey of Finland

Lodemann M, Fritz P, Wolf M, Ivanovich M, Hansen BT, Nolte E (1998) On the origin of saline fluids in the KTB (Continental Deep Drilling Project of Germany). Appl Geochem 13(5):651–671

Luukas J, Kousa J, Nironen M, Vuollo J (2017) Major stratigraphic units in the bedrock of Finland, and an approach to tectonostratigraphic division. Bedrock Finl Scale 1(1):000

Nurmi PA, Kukkonen IT, Lahermo PW (1988) Geochemistry and origin of saline groundwaters in the Fennoscandian Shield. Appl Geochem 3(2):185–203

Papp DC, Baciu C, Turunen K, Kittilä A (2021) Applicability of selected stable isotopes to study the hydrodynamics and contaminant transport within mining areas in Romania and Finland. Geol Soc Lond Spec Publ 507(1):169–192. doi.org/10.1144/SP507-2020-87

Papp DC, Larkins C, Turunen K, Cociuba I, Baciu C, Cozma A, Lazar L, Pop IC, Roba C, Mänttäri I, Nieminen S, Lahaye Y, Hendriksson N, Forsman P (2018) Geochemical and Isotope Methods for Assessing Contaminant Transport at Three Mine Sites: Kittilä mine in Finland and Roșia Montană and Zlatna mines in Romania. https://tupa.gtk.fi/raportti/arkisto/89_2018.pdf

Pellicori DA, Gammons CH, Poulson SR (2005) Geochemistry and stable isotope composition of the Berkeley pit lake and surrounding mine waters, Butte, Montana. Appl Geochem 20(11):2116–2137. doi.org/10.1016/j.apgeochem.2005.07.010

Phillips FM, Bentley HW (1987) Isotopic fractionation during ion filtration: I. Theory. Geochim Cosmochim Acta 51(3):683–695

Seal RR, Alpers CN, Rye RO (2000) Stable isotope systematics of sulfate minerals. Rev Mineral Geochem 40(1):541–602

Singh R, Venkatesh AS, Syed TH, Surinaidu L, Pasupuleti S, Rai SP, Kumar M (2018) Stable isotope systematics and geochemical signatures constraining groundwater hydraulics in the mining environment of the Korba Coalfield, Central India. Environ Earth Sci 77(15):1–17

Walton-Day K, Poeter E (2009) Investigating hydraulic connections and the origin of water in a mine tunnel using stable isotopes and hydrographs. Appl Geochem 24(12):2266–2282

Warr O, Giunta T, Onstott TC, Kieft TL, Harris RL, Nisson DM, Lollar BS (2021) The role of low-temperature 18O exchange in the isotopic evolution of deep subsurface fluids. Chem Geol 561:120027

Figure captions

Figure 1. Geochemical processes affecting the hydrogen and oxygen isotope composition of water (Clark and Fritz 2013). The Global Meteoric Water Line (GMWL) describes the global annual average relationship between hydrogen and oxygen isotope ratios in natural meteoric waters (Craig 1961).

Figure 2. (a) Regional geology map of the Kittilä mine (agnicoeagle.com) and (b) schematic diagram of the geology at Kittilä**.**

Figure 3. Chemical composition of water samples as a function of ionic strength (a) and depth (b). The marker shapes represent different types of water sample (see legend). Thin and thick marker edges represent samples collected in 2015 and 2021, respectively. Missing values for depth or ionic strength are shown with black markers. In the legend, GW and UG stand for groundwater and underground, respectively. For clarity, a simplified version of the relationship between sample types and chemical types is shown in the legend.

Figure 4. Cl (a), sulfate (b), H_2S (b) and Mn (d) concentration (mg/L) and calcite (e) and gypsum (f) saturation index as a function of depth and northing along the Kiistala shear zone. Grey lines show the pits and underground mine development. The marker shapes represent different types of water sample (see legend). Thin and thick marker edges represent samples collected in 2015 and 2021, respectively. Missing concentration values are shown with black markers. In the legend, GW and UG stand for groundwater and underground, respectively. For clarity, a simplified version of the relationship between sample types and chemical types is shown in the legend.

Figure 5. Hydrogen and oxygen isotope composition of water samples as a function of Cl (a) and sulfate (b) concentration compared to the GMWL (full line), the evaporation model of Craig (1961) (dashed line), the evaporation model of Gonfiantini (1986) (grey lines) and a mixing model between melted ice and water (Lehmann and Siegenthaler 1991) (orange lines). The values referred as f, h and m represent the evaporation rate (%), the relative humidity (%), and the mixing fraction of melted ice (%), respectively. The marker shapes represent different types of water sample (see legend). Thin and thick marker edges represent samples collected in 2015 and 2021, respectively. In the legend, GW and UG stand for groundwater and underground, respectively. For clarity, a simplified version of the relationship between sample types and chemical types is shown in the legend.

Figure 6. Distance of water isotope composition from the Global Meteoric Water Line as a function of sulfate concentrations. The marker shapes represent different types of water sample (see legend). Thin and thick marker edges represent samples collected in 2015 and 2021, respectively. The distance of water isotope composition from the GMWL is calculated as a hypotenuse perpendicular to the GMWL and passing through the data point. Applying Pythagorean theorem: $d = \sqrt{(x_2 - x_1)^2 + (y_2 - y_1)^2}$ with x_2 and x_1 the $\delta^{18}O$ values of the side opposite to angle A and y_1 and y_2 the δD values of the side adjacent to angle A with angle A being tangent to the GMWL.

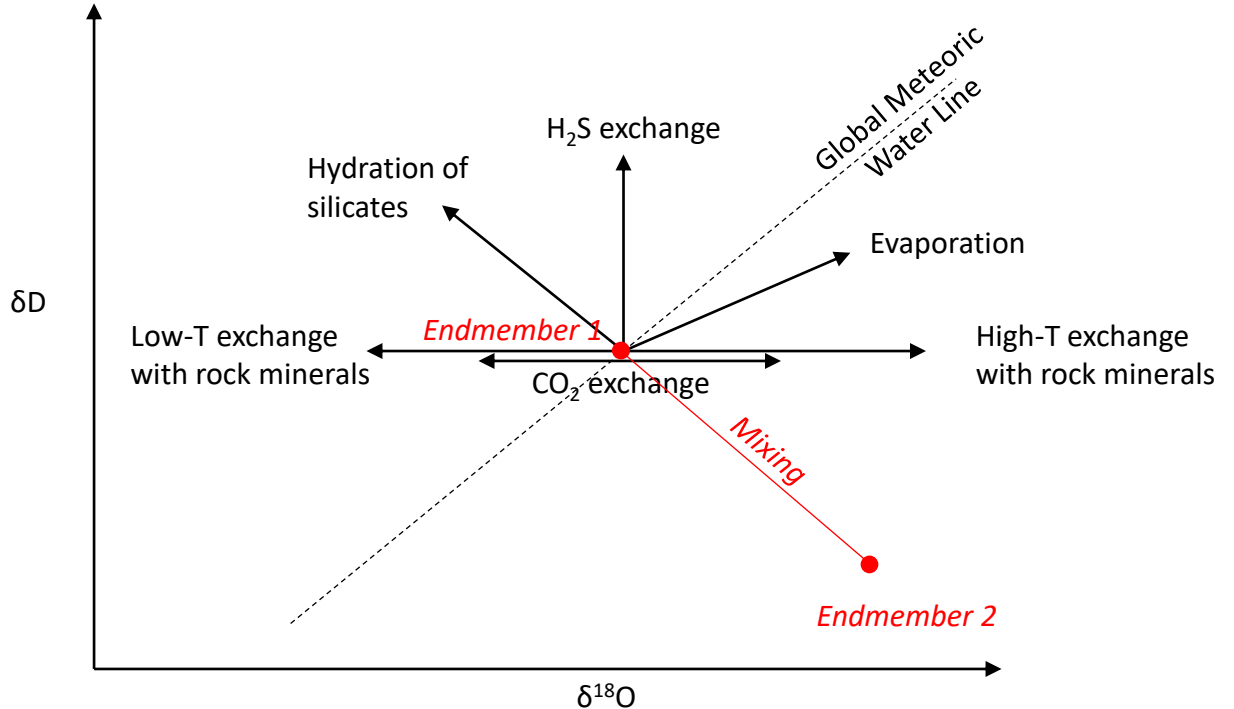
δD
δ18O
Global Meteoric Water Line
H2S exchange
Hydration of silicates
Evaporation
Endmember 1
Low-T exchange with rock minerals
High-T exchange with rock minerals
CO2 exchange
Mixing
Endmember 2

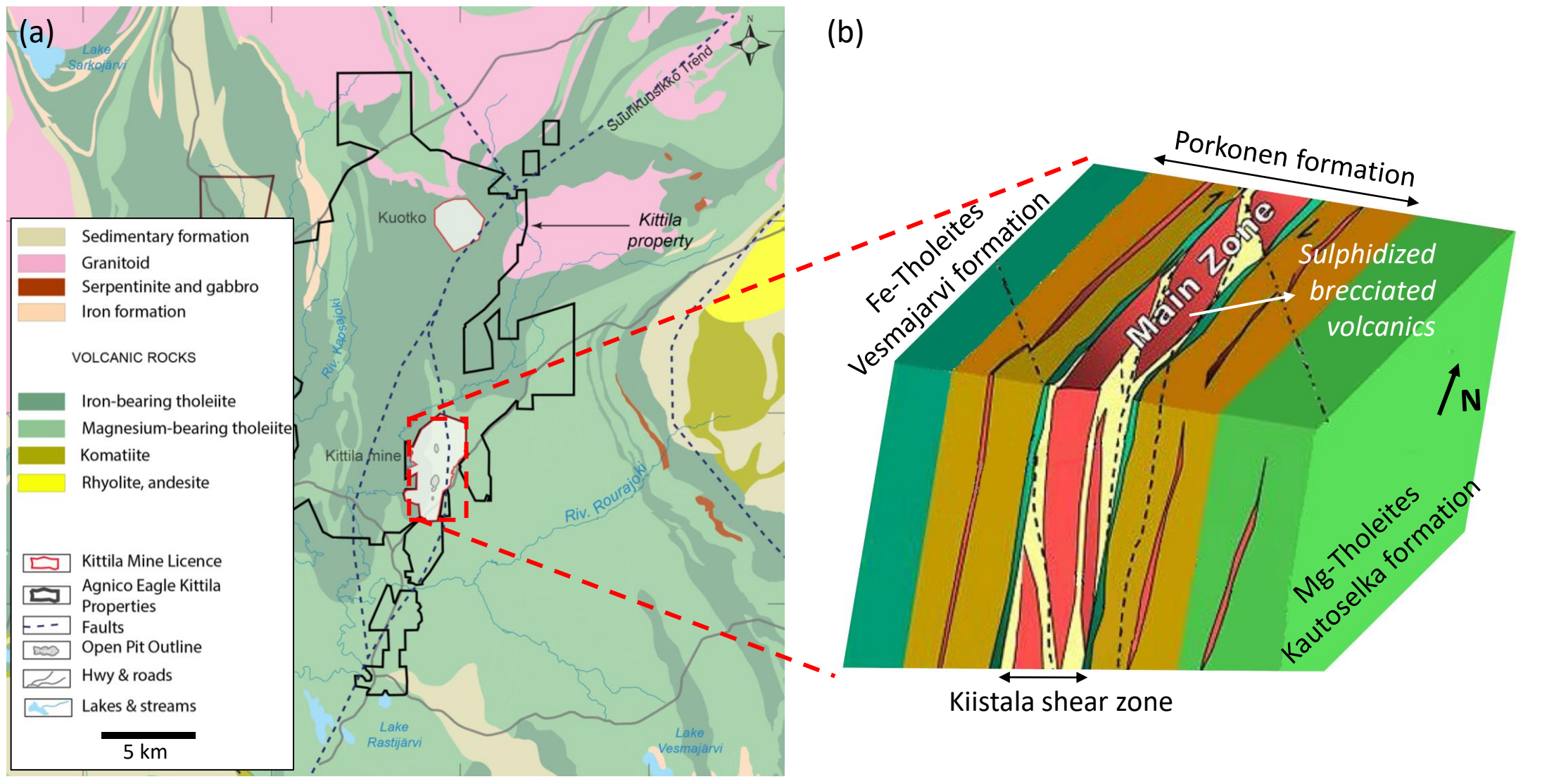
(a)
Lake Sarkojärvi
Suurikuusikko Trend
Kuotko
Kittila property
Riv. Kapsajoki
Kittila mine
Riv. Rourajoki
Lake Rastijärvi
Lake Vesmajärvi
Sedimentary formation
Granitoid
Serpentinite and gabbro
Iron formation
VOLCANIC ROCKS
Iron-bearing tholeiite
Magnesium-bearing tholeiite
Komatiite
Rhyolite, andesite
Kittila Mine Licence
Agnico Eagle Kittila Properties
Faults
Open Pit Outline
Hwy & roads
Lakes & streams
5 km
(b)
Porkonen formation
Fe-Tholeites
Vesmajarvi formation
Main Zone
Sulphidized brecciated volcanics
N
Mg-Tholeites
Kautoselka formation
Kiistala shear zone

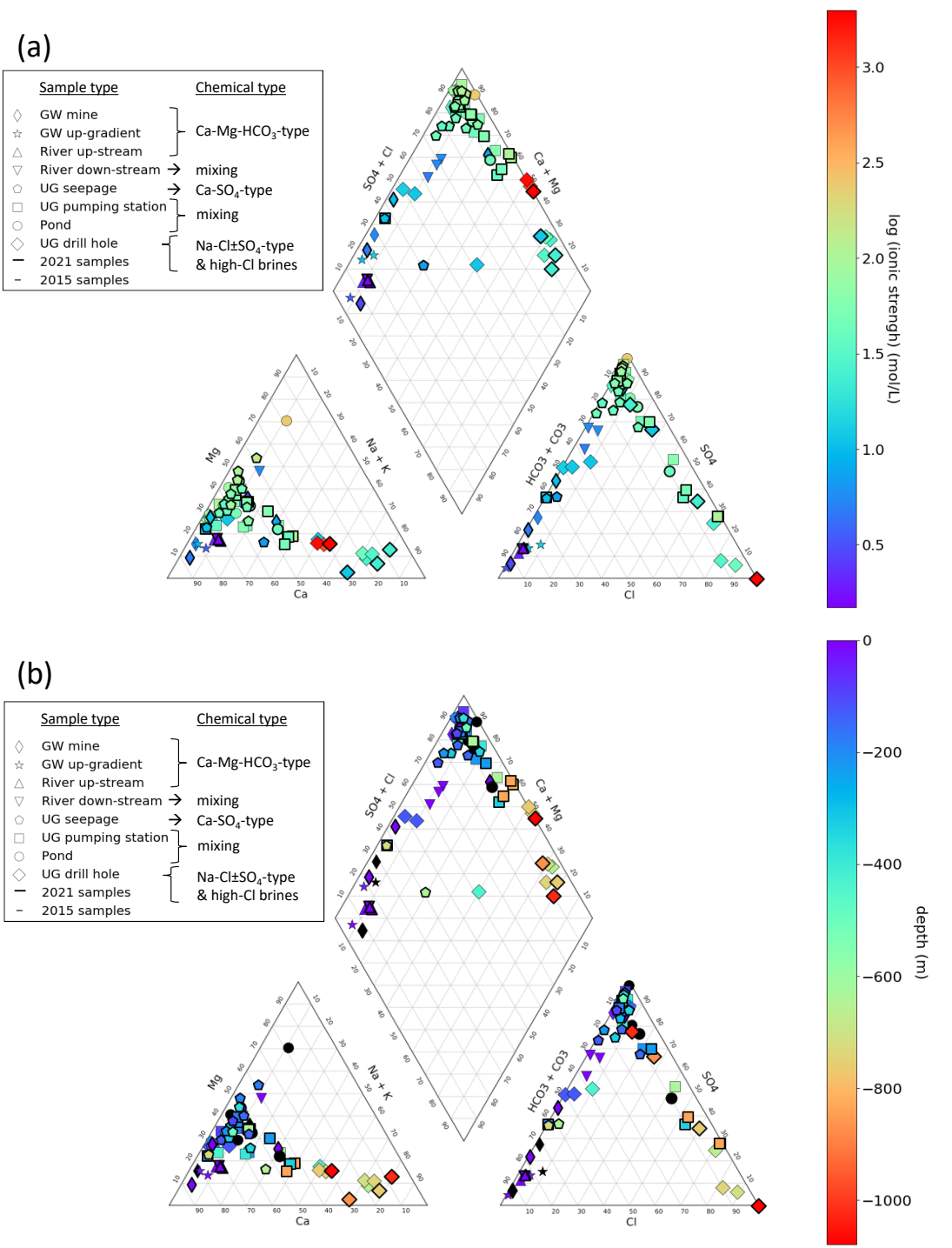
(a)
Sample type
Chemical type
GW mine
GW up-gradient
River up-stream
Ca-Mg-HCO3-type
River down-stream
mixing
UG seepage
Ca-SO4-type
UG pumping station
Pond
mixing
UG drill hole
2021 samples
2015 samples
Na-Cl±SO4-type & high-Cl brines
SO4 + Cl
Ca + Mg
Mg
Na + K
Ca
HCO3 + CO3
SO4
Cl
log (ionic strengh) (mol/L)
3.0
2.5
2.0
1.5
1.0
0.5
(b)
Sample type
Chemical type
GW mine
GW up-gradient
River up-stream
Ca-Mg-HCO3-type
River down-stream
mixing
UG seepage
Ca-SO4-type
UG pumping station
Pond
mixing
UG drill hole
2021 samples
2015 samples
Na-Cl±SO4-type & high-Cl brines
SO4 + Cl
Ca + Mg
Mg
Na + K
Ca
HCO3 + CO3
SO4
Cl
depth (m)
0
−200
−400
−600
−800
−1000

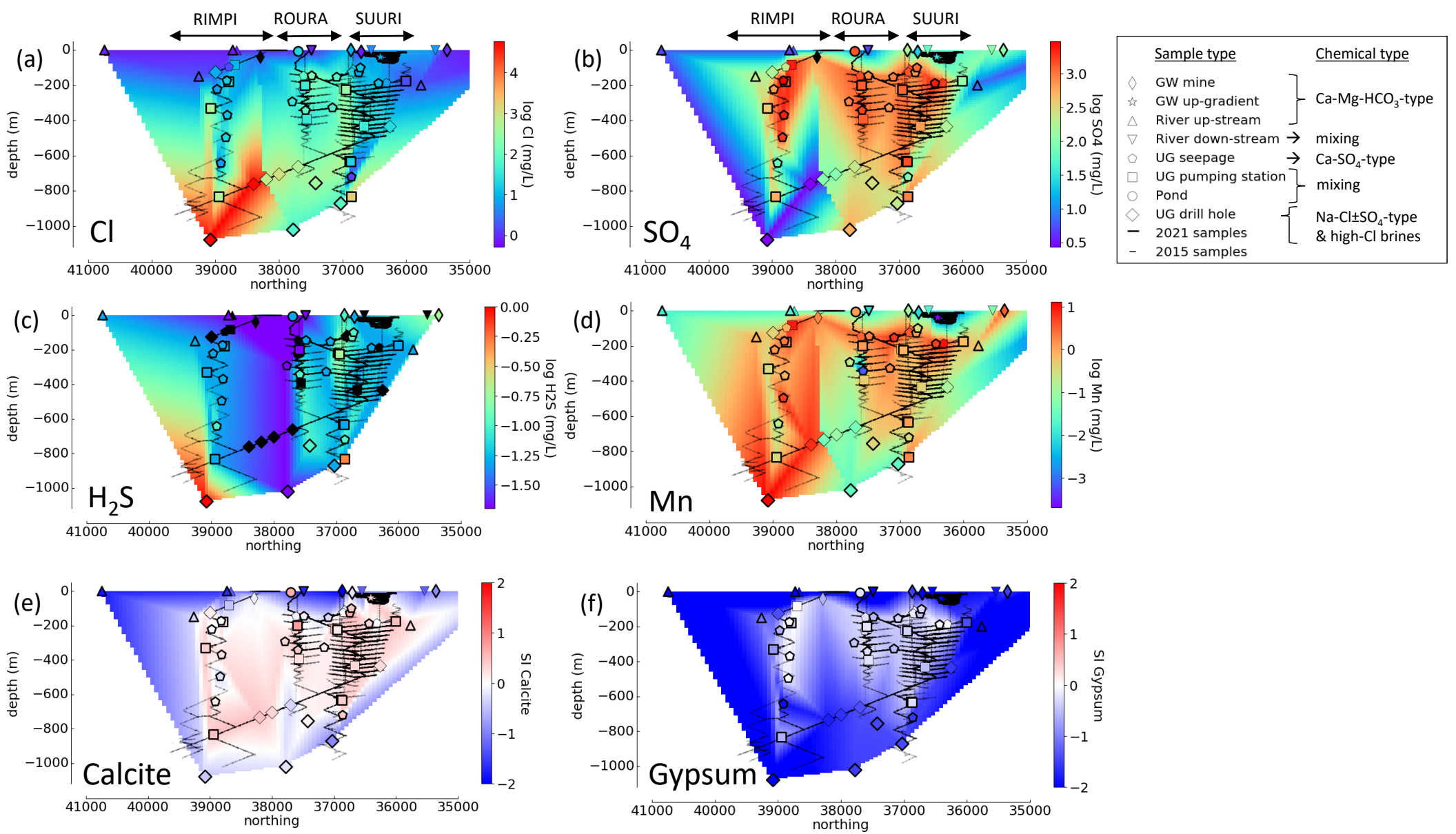
RIMPI
ROURA
SUURI
(a)
Cl
depth (m)
northing
log Cl (mg/L)
(b)
SO4
log SO4 (mg/L)
(c)
H2S
log H2S (mg/L)
(d)
Mn
log Mn (mg/L)
(e)
Calcite
SI Calcite
(f)
Gypsum
SI Gypsum
Sample type
Chemical type
GW mine
GW up-gradient
River up-stream
River down-stream
UG seepage
UG pumping station
Pond
UG drill hole
2021 samples
2015 samples
Ca-Mg-HCO3-type
mixing
Ca-SO4-type
mixing
Na-Cl±SO4-type
& high-Cl brines

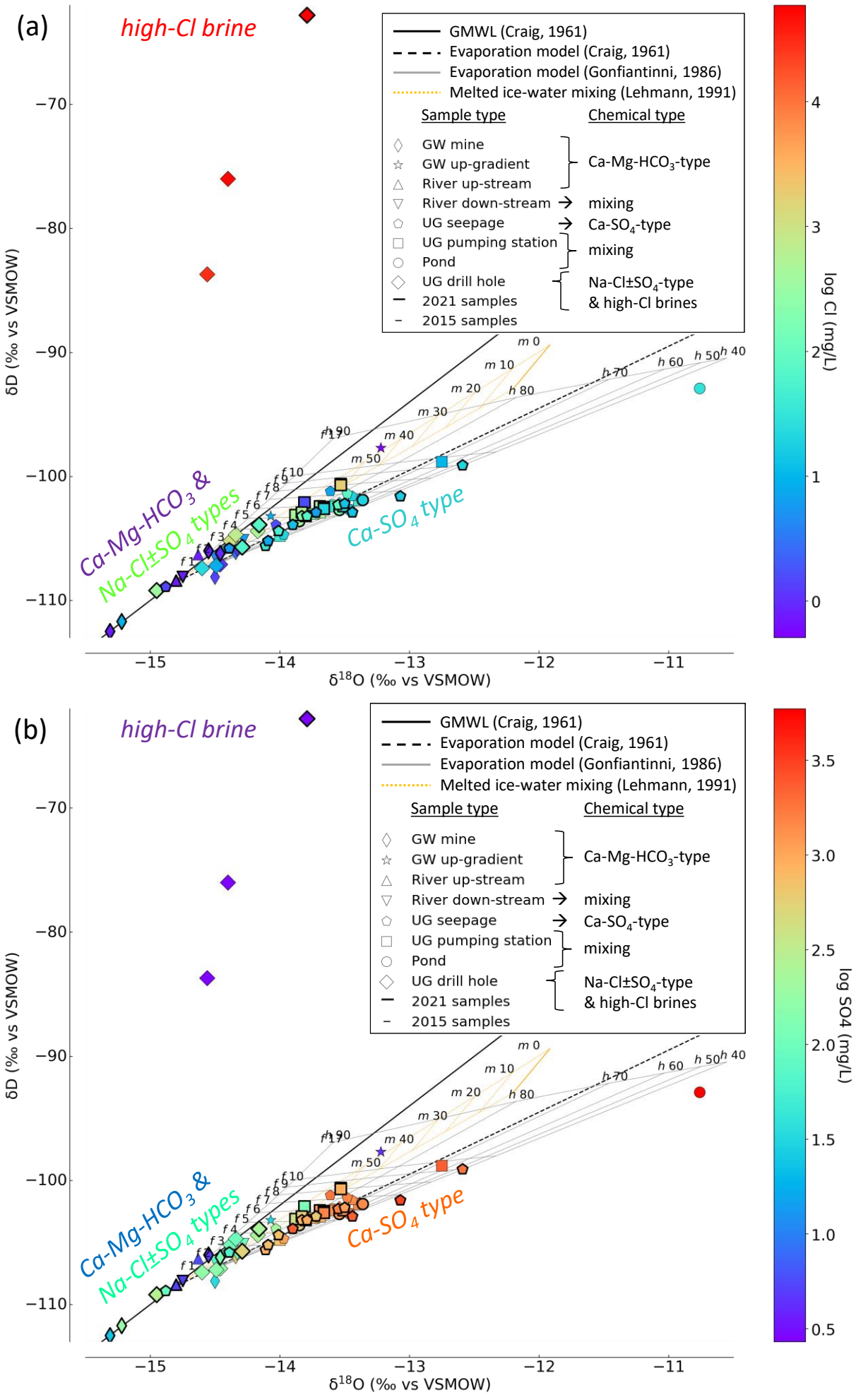
(a)
high-Cl brine
GMWL (Craig, 1961)
Evaporation model (Craig, 1961)
Evaporation model (Gonfiantinni, 1986)
Melted ice-water mixing (Lehmann, 1991)
Sample type
Chemical type
GW mine
GW up-gradient
River up-stream
Ca-Mg-HCO3-type
River down-stream
mixing
UG seepage
Ca-SO4-type
UG pumping station
Pond
mixing
UG drill hole
2021 samples
2015 samples
Na-Cl±SO4-type & high-Cl brines
Ca-Mg-HCO3 & Na-Cl±SO4 types
Ca-SO4 type
δD (‰ vs VSMOW)
δ18O (‰ vs VSMOW)
log Cl (mg/L)
(b)
high-Cl brine
log SO4 (mg/L)